

# Competitive binding of ribavirin, velpatasvir, and remdesivir to the active site of DNA polymerase can make them repurposable drugs to combat Monkeypox

<sup>1</sup>Shahjahan, <sup>2</sup>Joy Kumar Dey, <sup>3</sup>Sanjay Kumar Dey

<sup>1</sup>Dr. B. R. Ambedkar Center for Biomedical Research (ACBR), University of Delhi, Delhi-110007, INDIA;

<sup>2</sup>Central Council for Research in Homoeopathy, Ministry of AYUSH, Govt. of India, New Delhi-110058, Delhi, INDIA

<sup>3</sup>Dr. B. R. Ambedkar Center for Biomedical Research (ACBR), University of Delhi, Delhi-110007, INDIA

<sup>3</sup>Delhi School of Public Health, Institute of Eminence (IoE), University of Delhi, Delhi-110007, INDIA

**Abstract:** Inhibition of Monkeypox (MP) viral (MPV) DNA polymerases (DNAP or MP-DNAP) could help the treatment of MPV since these enzymes are essential for its replication. Thus, 90 small molecule antivirals (FDA approved: 75 and investigational: 15) from DrugBank have been virtually screened using two software (i.e., SwissDock and Schrodinger Inc.) against a recently solved cryo-EM structure of MP-DNAP (PDB ID: 8HG1). Current molecular interaction study has revealed that out of the docked 90 antivirals, ribavirin (-9.11/8.92 kcal/mol), velpatasvir (-10.38/-9.66 kcal/mol), and remdesivir (-9.39/-9.23 kcal/mol) can bind to the active site of MP-DNAP, with better efficacies than its substrates (i.e., dCTP (-7.17/-6.83 kcal/mol), dTTP (-7.22/-6.64 kcal/mol), dGTP (-7.48/-7.24 kcal/mol), and dATP (-7.36/-7.09 kcal/mol)). Present study has also unveiled that two WHO approved anti-monkeypox drugs, i.e., cidofovir (-8.46/-8.69 kcal/mol), tecovirimat (-7.7/-7.61 kcal/mol) etc.) could also interact at the substrate binding site of MP-DNAP. These three newly identified antiviral-small molecules as well as cidofovir and tecovirimat could not only interact/bind at the active site residues ASP549, TYR550, ASN551, SER552, LEU553, TYR554, PRO555, ASN665, TYR668, and ASP753 but also, they bind/formed multiple interactions at the active site Mg<sup>2+</sup>. Therefore, ribavirin, velpatasvir, and remdesivir can plausibly inhibit the substrate/nucleotide binding of MP-DNAP. Since all of these three lead drugs are FDA-approved, they can be directly tested in the MPV infected vero-cells and then undergo clinical trial if cell-based results are promising. Molecular mechanistic studies of complex of all the docked drugs bound to MP-DNAP using Prime-MMGBSA have further confirmed the tight interaction of the best three drugs as revealed by free energy calculations. These three drugs can be repurposed as antivirals against MPV, that may save thousands of human lives, and prevent any future viral epidemics, zoonotic transmissions etc.

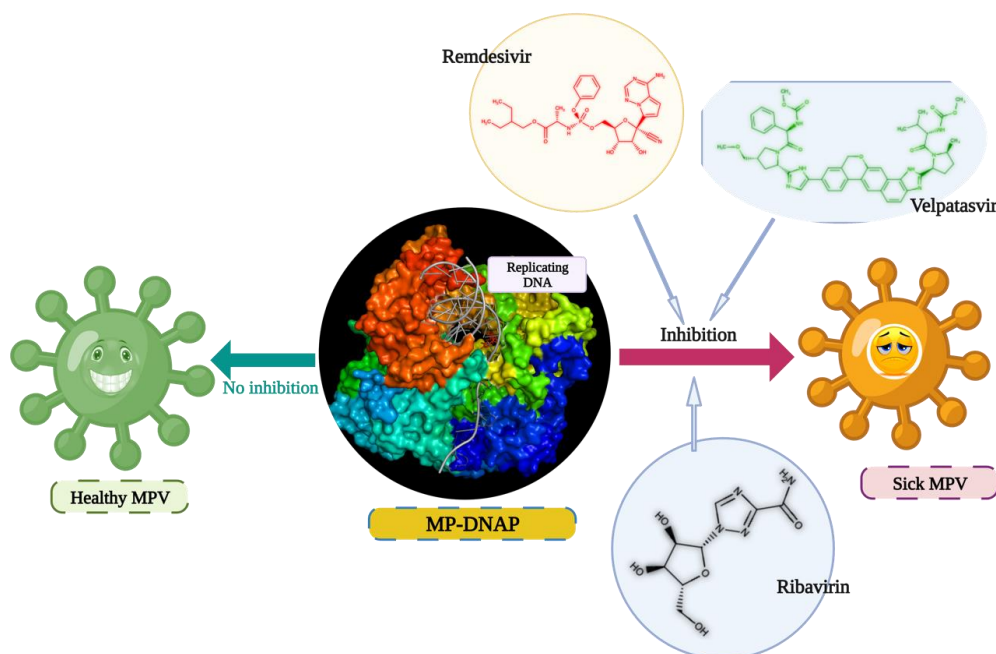
**Keywords:** MPV, DNAP, FDA-approved antivirals, ribavirin, velpatasvir, and remdesivir

## 1. Introduction

Monkeypox virus (MPV) causes monkeypox infection which was originally isolated and discovered from cynomolgus monkeys from a laboratory [1, 2]. MPV is from the Orthopoxviruses with family Poxviridae. Many famous viruses like Cowpox (CPXV), Variola (VARV), and Vaccinia (VACV) also belong to the same family [3-5]. Although MPV infection is not a new disease, it is grasping the world at an alarming speed [6-8]. This in turn indicates the present world population is almost unexposed to the virus and thus no immune response exists. Moreover, individuals who had been previously infected with Small Pox, are seen to be less prone to develop the MVP infection probably because both of them belong to the same viral family [9]. Therefore, MPV infection is a threat to this immune naïve population across the world [10]. Symptoms of MPV infection are just like smallpox, however with specific localization of pustular rash distribution and drastically reduced death rates [11]. MPV infection can be diagnosed using RT-PCR, cell (and/or tissue) culture, transmission/scanning electron microscopy, and IHC including ELISA, and Western Blot [12]. MPV genomic material is a double-stranded DNA with a length of 197 kb [13, 14]. MPV has an E9L gene-encoded DNA polymerase (DNAP) that is responsible for the DNA replication machinery and is well-characterized in other viruses in the same family [15-17]. Thus, DNAP and RNA polymerases of various viruses are one of the major targets to discover antiviral agents [18-22]. One year back, the world health organization (WHO) announced monkeypox outbreak as a public health emergency with concerns for the globe [6, 23, 24] which forced to speed up identification of new drugs and drug targets to combat the infection since available vaccines were not as effective as required to eliminate the disorder. Recently, Qi Peng et al., 2023 have solved the first ever structure of the MP-DNAP using cryo-EM [25]. Thus, combining the availability of MP-DNAP experimental structure (PDB ID: 8HG1) as a lucrative drug target and available FDA-approved antiviral drugs to attempt repurpose, current study applied virtual screening-based docking studies and finally in depth molecular mechanical analyses to identify antiviral molecules against MPV infection. Several such studies could lead to successful invention of a number of antiviral or therapeutic molecules in the recent past [22, 26-32]. As per WHO's guidelines, two existing drugs namely, tecovirimat (TPOXX or ST-246), and cidofovir are being prescribed to combat MPV infections [6, 11]. However, their mechanism of action is still not experimentally proven which has thus been attempted to investigate in the current study. Kumari et al., 2022 could also try to identify inhibitors of MPV, off course using *in silico* model of MP-DNAP [24] which thus need further experimental validation. Moreover, those molecules are not FDA-approved yet and thus needs rigorous preclinical and clinical trials before they can be developed as anti-MPV drugs, even if they show suitable efficacy. Thus, in the current study we have screened existing antiviral drugs which are already approved by FDA, with a

goal to repurpose them against MPV-DNAP. This will not need the lengthy preclinical and clinical trials to test their ADMET profile but only need to evaluate them directly against MPV infected cell lines, animal model, followed by testing them in MPV patients. This will not only reduce the cost of drug development but also significantly reduce the time required to obtain a drug rapidly as an alternate to ineffective or partially effective existing vaccines for MPV. From the current study, we have identified three FDA-approved antiviral drugs to bind at the active site of MPV-DNAP cryo-EM structure and thereby found to be potential inhibitor for the same. These three drugs can be repurposed to combat MPV infection. In the current study, we could also decipher the mechanism of action of the two WHO-approved anti-MPV drugs, namely, cidofovir and tecovirimat.

### Graphical abstract



## 2. Materials and Methods

### 2.1. Protein preparation using cryo-EM structure of MPV-DNAP

Schrodinger Inc.'s protein preparation wizard was used to refine, energy minimize, and add charges to make it compatible for docking using Glide XP [33] and SwissDock (<http://www.swissdock.ch>). Briefly, to refine, the cryo-EM structure was downloaded in the .pdb format and assigned bond orders to the structure, while skipping residues with existing double & triple bonds; added hydrogens to the structure; identified and treated metal ( $Mg^{2+}$ ) in the structure; created disulfide bonds; found 12 hetero groups and generated ionization/tautomeric states for all hetero groups; structure was optimized at pH 7.0 (using PROPKA); structure was energy minimized and resulted in an insignificant change in RMSD with the original structure as expected.

### 2.2. Source of ligands and their preparation

A total of 90 FDA-approved and 12 investigational antivirals (**Table 1**) were downloaded from DrugBank (<https://go.drugbank.com/unearth/q?searcher=drugs&query=antivirals>) and PubChem (<https://pubchem.ncbi.nlm.nih.gov/>) in .sdf format, while two WHO-approved anti-MPV drugs namely, tecovirimat, and cidofovir as well as its four substrates namely, dCTP, dTTP, dATP, and dGTP were downloaded from ChemSpider (<http://www.chemspider.com/>) as .mol format and all of them were finally converted to .mol2 extension using UCSF Chimera [34] prior to docking using SwissDock (<http://www.swissdock.ch>). To dock them in the Schrodinger Inc. [35], these ligands were further prepared using the ligprep module using the academic access license for one-month free trial to generate all possible isomers, tautomers, enantiomers or pH dependent alternative conformations. Briefly, the protocol used -max\_output: 32; -max\_generated conformations: 1024; neutralizer.py: -retain\_lab; -m: 200; epik.py: -pH 7.0; -retain\_i\_lab; -retain\_t\_lab; -tn: 8; stereoizer.py: 32.

### 2.3. Molecular interaction studies using docking tools

Best binding energies and interaction sites of the ligands were evaluated using two independent docking software: SwissDock [36], a freely available software and Schrodinger Inc. [35] which is a commercially available software but we got its academic

evaluation license for a month to complete the current work. Prior to docking experiment both protein, i.e. MP-DNAP (PDB ID: 8HG1) and all the ligands were minimized using CHARMM forcefield [37]. In case of SwissDock, dockings were conducted using the appropriate default parameters of the server to complete blind docking. Parameters used: wanted conformations: 5000; non-bonded facts evaluations: 5000; non-bonded seeds: 250; SwissDock steps: 100; ab-initio restrain steps: 250; clustering radius: 2.0 Å; maximum cluster size: 8. Once the results obtained, they were further analyzed critically using UCSF Chimera [34] to find out the binding site and the amino acids responsible for such interactions.

For glide XP docking using Schrodinger Inc., the cryo-EM structure of MP-DNAP was initially prepared using above-mentioned method. Then, a receptor grid was prepared in X, Y, and Z coordinates as follows: grid center 133.86, 149.36, 149.29; inner box 40, 40, 40; outer box 76, 76, 76. Glide XP docking was used for docking the small molecule antivirals, WHO-approved two anti-MPV drugs, and substrates against the MP-DNAP cryo-EM structure. Briefly, the Glide XP (Extra Precision) protocol was: buried polar penalty: 0.000; Coulomb vdW cutoff: 0.000; H bond cutoff: 0.000; Metal-ligand cutoff: 10.000; assign GlideScore XP5.0 parameters; Glide Extra Precision mode used maxref = 800; grow mode-t; Lig-maecharges: true; poses per ligand: 4.

Initial docking protocol was validated by docking dTTP to MP-DNAP and the obtained RMSD between docked and the experimental conformations was insignificantly small, 0.2 Å. It also confirmed the binding site as reported in the experimental structure.

## 2.4. Generation of molecular interaction maps:

Two dimensional protein-ligand interaction maps for the best three antivirals, positive control drugs, and substrates of MP-DNAP were generated using the visualization software Maestro available with Schrodinger Inc. [35]. Similarly, three-dimensional interaction maps of the protein-ligand complexes were made by UCSF Chimera [34], PyMol [38] and Maestro module of Schrodinger Inc. [35] in both ribbon and surface views.

## 2.5. MM-GBSA and free energy studies to evaluate the drug-MP-DNAP complex at the molecular mechanistic level:

All docked antivirals, cidofovir, tecovirimat as well as the substrates of MP-DNAP bound to the protein, i.e., MP-DNAP-drug complexes, were further evaluated using the Prime MMGBSA module of the Schrodinger Inc. and parameters like receptor strain, ligand strain, MMGBSA dG Bind etc. were calculated. By using Prime-MM-GBSA module, current study calculated the binding energies of the ligands bound to MP-DNAP employing their corresponding docked complex structures obtained after docking using glide XP method as described above [39, 40].

Binding affinity of inhibitors in the binding site of a protein like MP-DNAP was calculated by using Prime-MM-GBSA method by with the help of Prime MMGBSA module of Schrodinger Inc. [39, 40]. It calculates a diverse array of energy properties/parameters. This include energies for the drug (ligand), target-receptor, and ligand-protein complex structures plus the difference in energy between the strain and the binding, and are divided into contributions from several energy parameters as described below. The key-five basic energy calculations are: (1) Optimized free receptor (="Receptor"); (2) Optimized free ligand (="Ligand"); (3) Optimized complex (="Complex"); (4) Receptor from minimized/optimized complex; (5) Ligand from minimized/optimized complex; (6) From these energies, the following strain and binding energies are calculated:

Rec Strain = Receptor (from optimized complex) – Receptor ..... equation 1

Lig Strain = Ligand (from optimized complex) – Ligand ..... equation 2

MMGBSA dG Bind = Complex – Receptor – Ligand ..... equation 3

MMGBSA dG Bind (NS) = Complex – Receptor (from optimized complex) – Ligand (from optimized complex) = MMGBSA dG Bind – Rec Strain – Lig Strain ..... equation 4

In the equation 4 above, NS: no strain; it is the binding/interaction energy without accounting for the receptor and ligand conformational changes needed to form the drug-MP-DNAP complex. Not only the total energy, but also the contributions to the total energy from various sub-energies is also reported which include: **Coulomb—Coulomb energy**; Covalent—Covalent binding energy; vdW—Van der Waals energy; Lipo—Lipophilic energy; Solv GB—Generalized Born electrostatic solvation energy; Energy—Total energy (Prime energy); Hbond—Hydrogen-bonding correction; Packing—Pi-pi packing correction; SelfCont—Self-contact correction. The property names shown in the Project Table have the form calculation-type\_component

where calculation-type is the structure, strain, or binding energy type (e.g., "Receptor", "Lig Strain", or "MMGBSA dG Bind") and component is the energy component from the table above.

### 3. Results

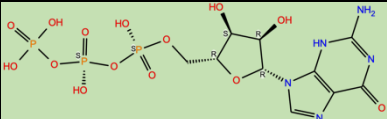
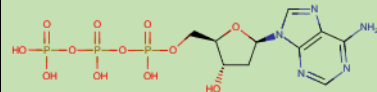
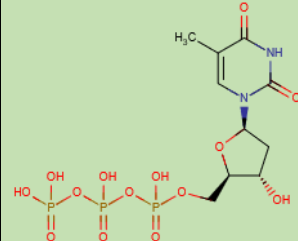
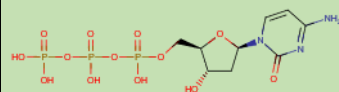
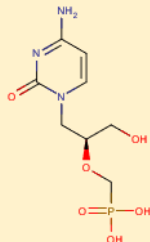
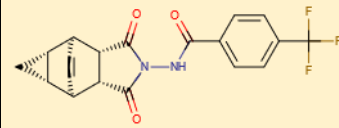
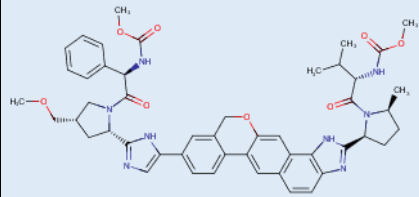
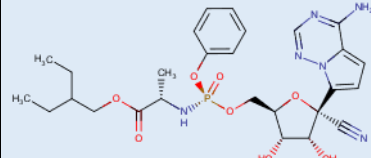
#### 3.1. Selection of FDA-approved antivirals for screening against MP-DNAP to repurpose them to treat Monkeypox:

Current study has selected 90 antivirals from DrugBank (<https://go.drugbank.com/unearth/q?searcher=drugs&query=antivirals>), out of which 75 drugs are FDA approved and 15 drugs are still under clinical trials (Table 1; Supplementary Table 1). With the status of the drugs as suitable for human consumption, the need to test toxicity of the drugs do not arise, and they can be easily repurposed for the prevention of MPV infection, provided they may bind to the MP-DNAP with high affinity. The chosen drugs were screened *in silico* in search of potential hits which can inhibit DNAP of MPV. In contrast to traditional docking studies, current study has employed two software, SwissDock (freely available) and Schrodinger Inc. (commercially available) to increase the stringency in selecting best small molecule antivirals which will be common in both the software/methodology. This in turn may identify stricter inhibitors of MP-DNAP thereby restricting the infection. WHO has recently advised cidofovir, and tecovirimat, for the treatment of MPV infection till the time there are no antiviral drugs which are specifically discovered/designed against the said virus [41]. Coincidentally, mechanism of action or the target proteins for these two WHO-advised drugs in the MPV is unknown and thus we tried find their interaction, if any, with MPV-DNAP as well. Initial docking protocols were validated by docking dTTP to the MPV-DNAP and the complex was superposed over the experimental complex to calculate RMSD between them, resulting in a low RMSD thereby validating the docking protocols. All docking results of the FDA-approved antivirals, investigational antivirals and cidofovir, tecovirimat bound to MP-DNAP were compared with the substrates of MP-DNAP, i.e., dATP, dCTP, dGTP, and dTTP, in terms of binding affinity and interaction sites.

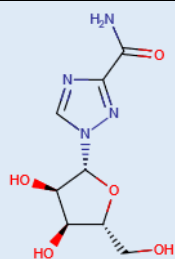
#### 3.2. Binding of dTTP to the active site of MP-DNAP validated the docking protocol and the same is further supported by binding of the three other substrates, dATP, dGTP, and dCTP to the enzyme:

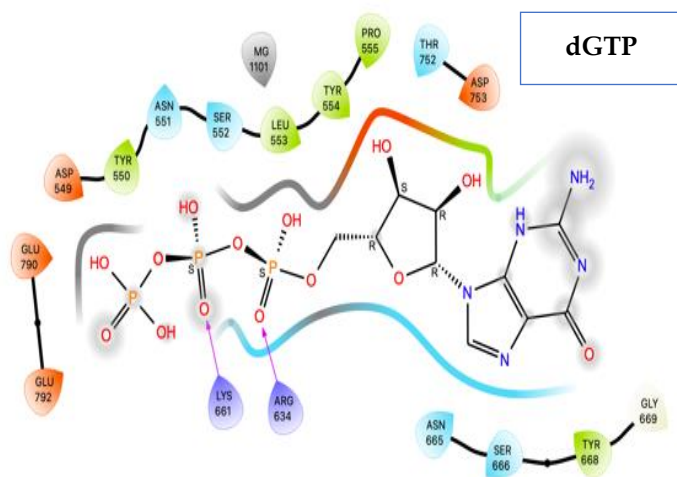
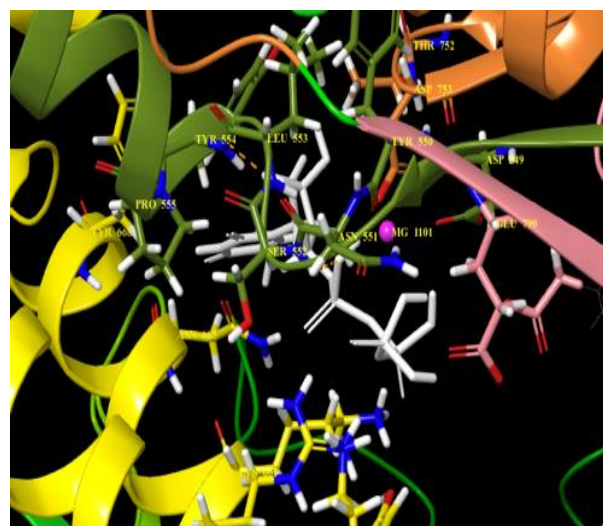
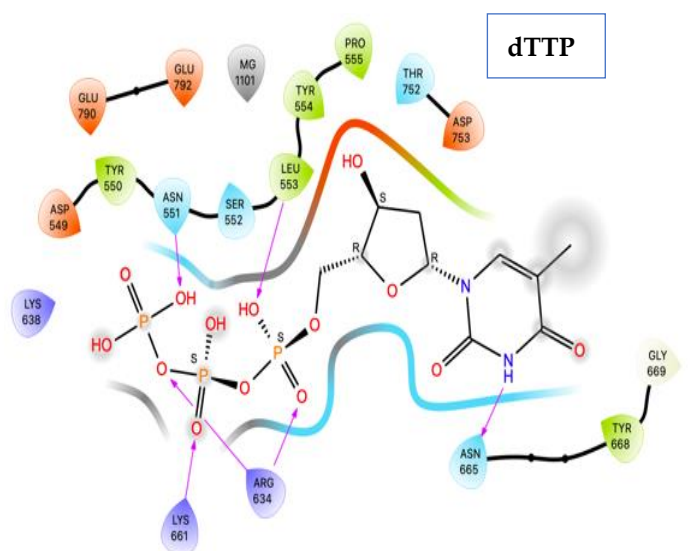
Just like any other DNA polymerases, MPV-DNAP has also four substrates, namely, dATP, dCTP, dGTP, and dTTP. MP-DNAP cryo-EM structure was solved experimentally in its substrate dTTP-bound state and thus initial docking protocols were validated by docking dTTP to the MPV-DNAP and the complex was superposed over the experimental complex to calculate RMSD between them. It resulted in an insignificant RMSD of 0.2 Å thereby validating the docking protocols and thus were further used for all other docking. Then, the three other substrates (i.e., dATP, dCTP, and dGTP) were also docked and compared with the solved dTTP-bound structure of MP-DNAP (PDB ID: 8HG1). All four substrate bound structures of the MP-DNAP further validated the docking protocols as explained here. From the current study, it was found that dTTP can bind to the active site of the MPV-DNAP and interact with Lys661, Arg634, Leu553, Asn551, Asn665 (Fig. 1, d, Supplementary Fig. 1, d) which is close to  $Mg^{2+}$ , cofactor of this enzyme. It not only showed a high binding energy of -7.22 kcal/mol (SwissDock) or -6.64 kcal/mol (Glide XP) for MPV-DNAP but also matched the binding site amino acid residues as shown in the solved cryo-EM structure of the enzyme (Table 1; Supplementary Table 1) [25]. It was further observed that dATP has a binding energy of -7.36 kcal/mol (SwissDock) or -7.09 kcal/mol (Glide XP); while dCTP, and dGTP have binding energies of -7.17 kcal/mol (SwissDock) or -6.83 kcal/mol (Glide XP) and -7.48 kcal/mol (SwissDock) or -7.24 kcal/mol (Glide XP), respectively for MP-DNAP (Table 1). All four of these substrates could show interaction with the active site consisting of ASP549, TYR550, ASN551, SER552, LEU553, TYR554, PRO555, ASN665, TYR668, and ASP753 as well its cofactor  $Mg^{2+}$  (Fig. 1, a-c; Fig. 3; Supplementary Fig. 1, a-c). It also indicates that substrate analogues or nucleoside analogues that can bind to MP-DNAP with higher affinity than the original substrate can be useful inhibitors of this enzyme. This study also indicates that dGTP has the highest affinity for the experimentally solved structure of MP-DNAP, followed by dATP>dTTP>dCTP (Table 1; Supplementary Table 1).

**Table 1: Binding energies and details of DNAP-substrates, cidofovir, tecovirimat, and top three FDA-approved antivirals, screened against MP-DNAP.**

Sl. No.	Antiviral Drug/Substrate Name	Structure	Binding energy from Swiss Dock (kcal/mol)	Binding energy (Glide score) (kcal/mol)
<b>Substrates of DNA polymerase</b>				
1	<a href="#">dGTP</a>		-7.48	-7.24
2	<a href="#">dATP</a>		-7.36	-7.09
3	<a href="#">dTTP</a>		-7.22	-6.64
4	<a href="#">dCTP</a>		-7.17	-6.83
<b>WHO-approved anti-MPV drugs</b>				
5	<a href="#">Cidofovir</a>		-8.46	-8.69
6	<a href="#">Tecovirimat</a>		-7.70	-7.61
<b>Top three MP-DNAP binding FDA-approved antivirals</b>				
7	<a href="#">Velpatasvir</a>		-10.38	-9.66
8	<a href="#">Remdesivir</a>		-9.39	-9.23



9	<u>Ribavirin</u>		-9.11	-8.92
---	------------------	---	-------	-------



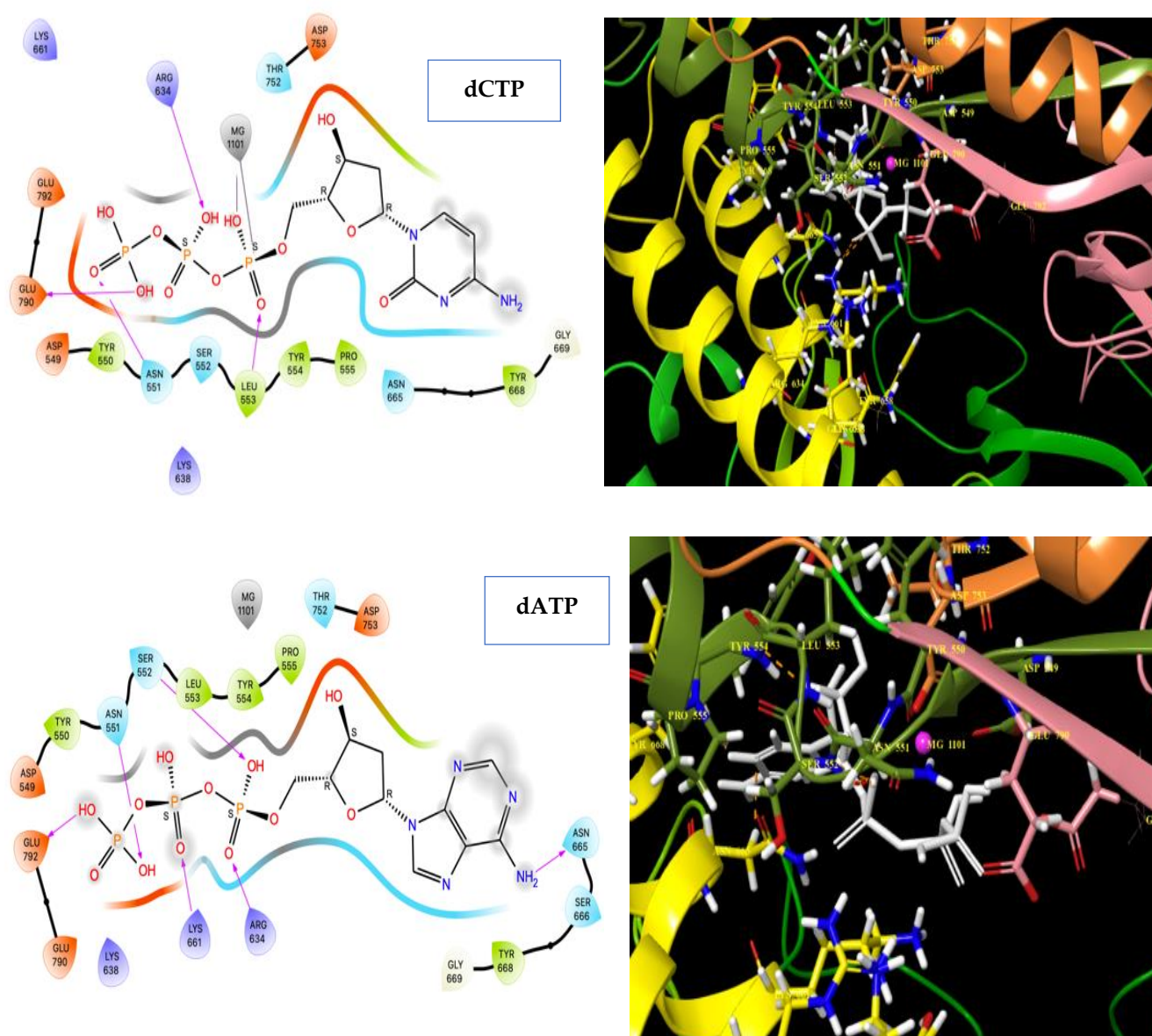


Figure 1: Four substrates docked to MP-DNAP (PDB ID: 8HG1). A) dATP, B) dCTP, C) dGTP and D) dTTP. Left-hand panel shows two-dimensional interaction maps between the substrates and MP-DNAP. Right-hand panel shows ribbon view of interaction highlighting all four substrates binding within the active site pocket of MP-DNAP via contact with key residues namely, ASP549, TYR550, ASN551, SER552, LEU553, TYR554, PRO555, ASN665, TYR668, and ASP753, as well as with  $Mg^{2+}$ . This finding validated our docking protocols.  $Mg^{2+}$  has been shown as a pink ball in the right-hand panel while as a black circle in the left-hand panel.

### 3.3. WHO-approved anti-MPV drugs cidofovir and tecovirimat interact with active site residues and the $Mg^{2+}$ of MP-DNAP:

In an attempt to search for binding sites of the two WHO-approved anti-MPV drugs, namely cidofovir and tecovirimat over MP-DNAP, these two drugs were also docked (Fig. 2, Fig. 3, Supplementary Fig. 2; Table 1; Supplementary Table 1). It was observed that cidofovir (-8.46/-8.69 kcal/mol) has higher affinity than tecovirimat (-7.7/-7.61 kcal/mol) for MP-DNAP (Table 1, Supplementary Table 1, Fig. 2, and Supplementary Fig. 2). Cidofovir and tecovirimat bind near the active site residues of MP-DNAP, namely, ASP549, TYR550, ASN551, SER552, LEU553, TYR554, PRO555, ASN665, TYR668, and ASP753 (Fig. 2, a & b). These two drugs also bind near the active site  $Mg^{2+}$ . Cidofovir forms H-bond with Arg634 and Tyr554; metal coordination with  $Mg^{2+}$ ; hydrophobic interaction with Tyr554; while tecovirimat forms H-bond with Leu553; metal coordination with  $Mg^{2+}$ ; pi-cationic interaction with Arg634 (Fig. 2, a & b; Supplementary Fig. 2). This is the first-time report of the binding site of these two WHO-approved anti-MPV drugs on its DNAP. However, these findings can further be validated by solving co-cryo-EM structure of these drug-bound MP-DNAP in future.



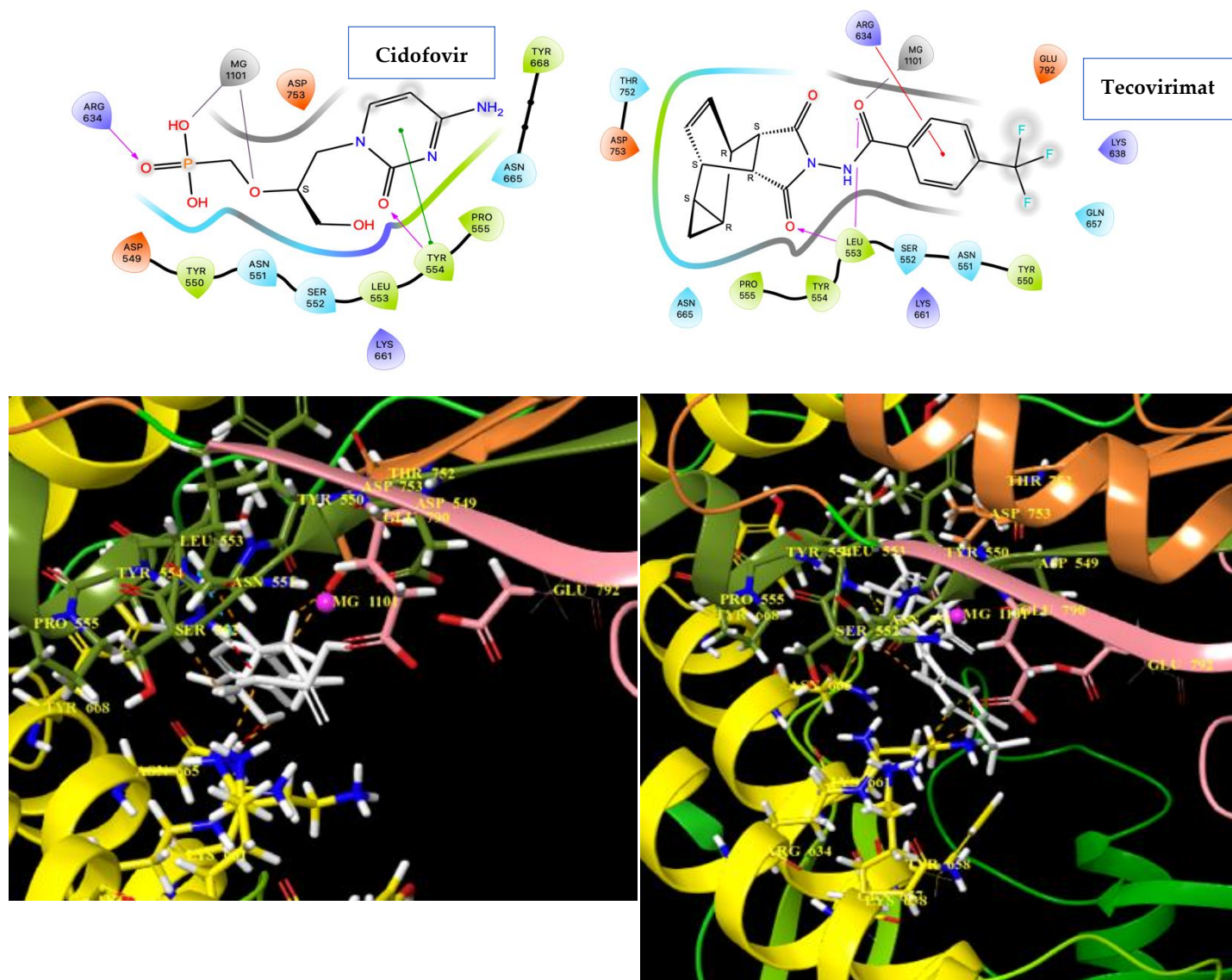
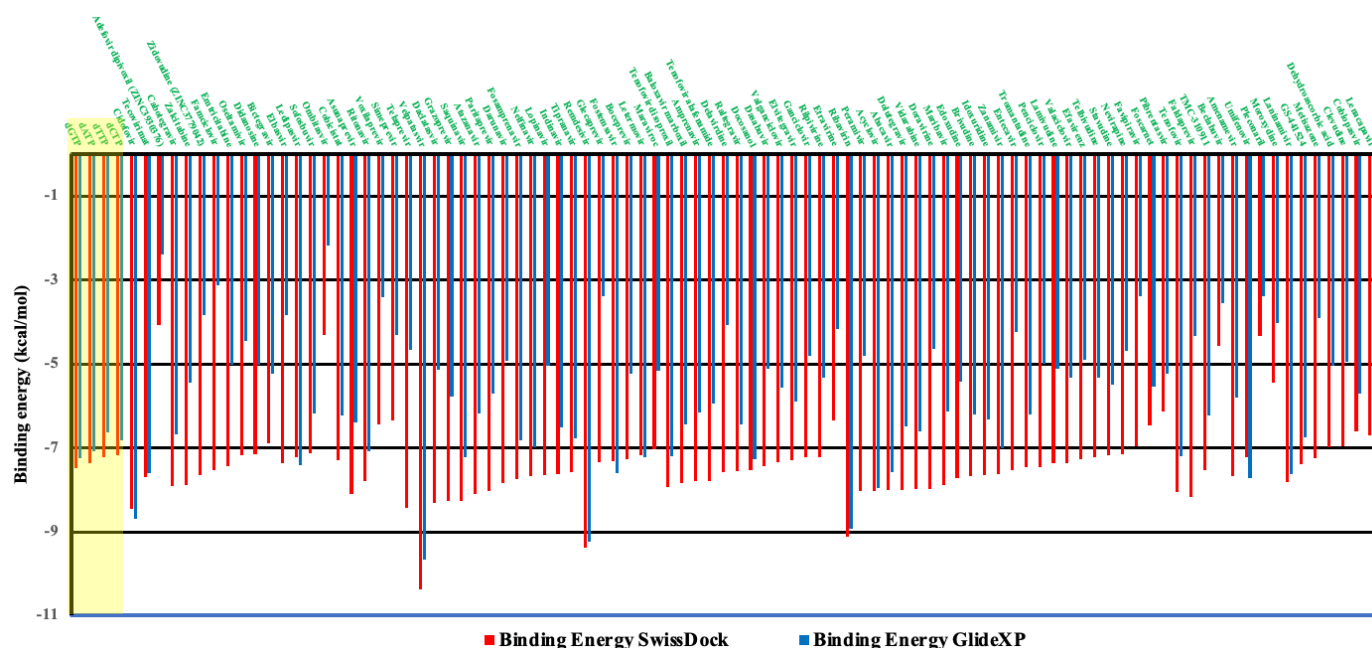


Figure 2: Two WHO-approved anti-MPV drugs, cidofovir and tecovirimat docked to MP-DNAP (PDB ID: 8HG1). A) cidofovir, and B) tecovirimat. Top panel shows two-dimensional interaction maps between the two WHO-approved anti-MPV drugs and MP-DNAP. Lower panel shows ribbon view of interaction highlighting both cidofovir and tecovirimat are again binding within the active site pocket of MP-DNAP just like its substrates, via contact with key residues namely, ASP549, TYR550, ASN551, SER552, LEU553, TYR554, PRO555, ASN665, TYR668, and ASP753, as well as with  $Mg^{2+}$ . This is the first report showing the interaction sites of cidofovir and tecovirimat to the experimental structure of MP-DNAP.  $Mg^{2+}$  has been shown as a pink ball in the lower panel while as a black circle in the top panel.





**Figure 3:** Bar graph representing the binding energies (kcal/mol) of the FDA-approved antivirals and WHO-approved anti-MPV drugs (cidofovir and tecovirimat) docked to MPV-DNAP (cryo-EM structure; PDB ID: 8HG1) estimated by SwissDock (red bars) and Glide XP (blue bars). Substrates of MP-DNAP, dATP, dCTP, dGTP, and dTTP are shown in transparent yellow box.

### 3.4. Ribavirin, velpatasvir, and remdesivir interact with active site residues and the $Mg^{2+}$ of MP-DNAP, indicating their plausible competitive mode of inhibition:

After docking the substrates of DNAP as well as cidofovir, tecovirimat, 90 antivirals obtained from the DrugBank were docked and their binding energies were tabulated in **Table 1** and **Supplementary Table 1**, shown in **Fig. 3** using bar graph to compare the results with the substrates. Out of these 90 antivirals, 75 are FDA-approved while 15 are still under clinical trial as detailed in **Table 1** and **Supplementary Table 1**. Only 12 drugs out of these docked 90 antivirals were found to bind at the active site of the MP-DNAP and showed better binding energies than the allosteric binders. It was also observed that among this active site binders, velpatasvir showed the highest affinity for MPV-DNAP with a binding energy of -10.38/-9.66 kcal/mol which was followed by remdesivir with a binding energy -9.39/-9.23 kcal/mol, and ribavirin with affinity of -9.11/8.92 kcal/mol (**Table 1**, **Fig. 3**). Importantly, these binding energies are much better than either substrate or cidofovir and tecovirimat, thereby velpatasvir, remdesivir, and ribavirin seem to be promising or better inhibitors than the known inhibitors of MPV that exists till date. Just like the substrates as well as cidofovir and tecovirimat, the newly identified best three antiviral-small molecules from the current study could also bind near the active site residues of MP-DNAP, namely, ASP549, TYR550, ASN551, SER552, LEU553, TYR554, PRO555, ASN665, TYR668, and ASP753 (**Fig. 4, a-c**). Binding site of these three leads also include the active site  $Mg^{2+}$ . Ribavirin, remdesivir, and velpatasvir could form one, two, and one interaction/s (**Fig. 4, a-c**; **Supplementary Fig. 3 a-c**; **Table 2**), respectively with the active site  $Mg^{2+}$  thereby making them tightly binding inhibitors of MP-DNAP than the existing ones till date. Ribavirin forms H-bond with Asn665; metal coordination with  $Mg^{2+}$ ; pi-cationic interaction with Lys661; while remdesivir forms H-bond with Asp753, Lys661, Leu553; metal coordination with  $Mg^{2+}$ ; velpatasvir forms H-bond with Asp753, Tyr497; metal coordination with  $Mg^{2+}$ ; pi-cationic interaction with Tyr554 (**Fig. 4, a-c**; **Supplementary Fig. 3 a-c**). All these finding indicate that these three FDA-approved drugs can probably block the entry of new-coming nucleotide and prevent MP-DNAP from replication thereby it can block the growth of MPV inside the host. Their interaction or blockade at the active site of MP-DNAP further indicates that they are plausibly inhibiting the enzyme in competitive mode with higher affinity than the substrates. Thus, findings of the current study can lead to rapid preclinical evaluation of these drugs in MPV-infected vero cell lines and/or animal models of MPV to finally enter into human trials, especially in the MPV patients to find their ultimate application against MPV infection. Remaining 87 antivirals obtained from the DrugBank could also show somewhat binding affinities with MP-DNAP as tabulated in **Supplementary Table 1** and shown graphically in **Fig. 3**, but they are neither better than the cidofovir, tecovirimat, nor than the substrates and many of them bind to allosteric sites as well.

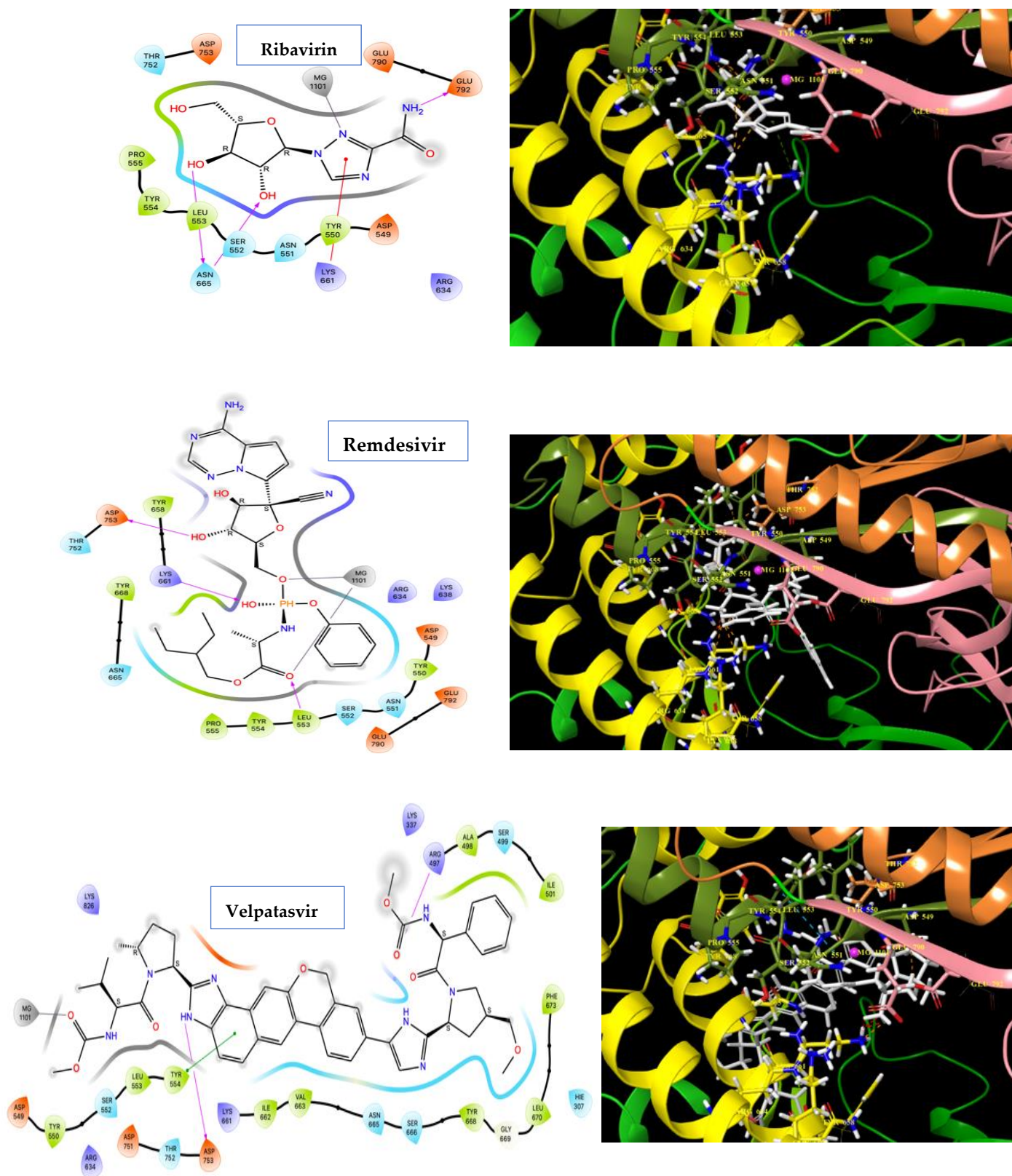


**Figure 4:** Three best hits namely, ribavirin, remdesivir, and velpatasvir docked to MP-DNAP (PDB ID: 8HG1). A) ribavirin, B) remdesivir, and C) velpatasvir. Left-hand panel shows two-dimensional interaction maps between the top three antiviral hits and MP-DNAP. Right-hand panel shows ribbon view of interaction highlighting that all three hit molecules too bind in the active site pocket of MP-DNAP just like its substrates and WHO-approved anti-MPV drugs, via contact with key residues namely, ASP549, TYR550, ASN551, SER552, LEU553, TYR554, PRO555, ASN665, TYR668, and ASP753, as well as with  $Mg^{2+}$ . This also suggests that ribavirin, remdesivir, and velpatasvir are probably competitively inhibiting MP-DNAP.  $Mg^{2+}$  has been shown as a pink ball in the right-hand panel while as a black circle in the left-hand panel.

**Table 2: Physico-chemical interactions of the best three hits of MP-DNAP.**

Drug and Its Chemical Structure	Hydrogen bonds/ Electrostatic interactions/ van der Waals interactions with MP-DNAP	No of interactions formed with Mg <sup>2+</sup> of MP-DNAP
<b>Ribavirin</b>	ASP549, TYR550, ASN551, SER552, LEU553, TYR554, PRO555, ASN665, TYR668, and ASP753	1
<b>Remdesivir</b>	ASP549, TYR550, ASN551, SER552, LEU553, TYR554, PRO555, ASN665, TYR668, and ASP753	2
<b>Velpatasvir</b>	ASP549, TYR550, ASN551, SER552, LEU553, TYR554, PRO555, ASN665, TYR668, and ASP753	1

### 3.5. MM-GBSA calculations of the antivirals confirmed tight binding of ribavirin, velpatasvir, and remdesivir to the target MP-DNAP:

While docking, that too with two different software cum algorithms could help the current study lead to stringent selection or identification of plausible best inhibitors of MP-DNAP from among the 90 FDA-approved antivirals, our previous studies [30] have shown that and additional molecular mechanistic study using MM-GBSA may further ascertain the outcome or binding affinities of the leads against their protein target. Thus, the receptor-ligand complexes, i.e. each of the 90 antiviral-MP-DNAP complexes as well as cidofovir-MP-DNAP, tecovirimat-MP-DNAP, and dCTP/dATP/dTTP/dGTP-MP-DNAP obtained after Glide-XP were evaluated using the Prime-MM-FBSA module of the Schrodinger Inc. and the key energy parameters with their calculated energy values are shown in **Supplementary Table 2 and in Table 3** for the best three leads. While, in case of docking ribavirin could show the best affinity for MP-DNAP (**Table 1**), Prime-MM-GBSA analyses of the docked complexes revealed that velpatasvir could stabilize the receptor-ligand complex partially better than the two others with a free energy for the complex formation (MMGBSA dG Bind (Coulomb)) as -74.64 kcal/mol, while remdesivir and ribavirin could make the complexes with energies of -64.71 kcal/mol and -40.94 kcal/mol (**Table 3; Supplementary Table 2**). Nevertheless, these findings confirm the tight binding of ribavirin, remdesivir, and velpatasvir with MP-DNAP thereby increasing confidence in the outcome of the current study to propose them for repurposable drugs to combat MPV infection.

**Table 3: Calculated free energies of the top three drugs bound to MP-DNAP using Prime-MM-GBSA.**

Types of energy	Free energies (kcal/mol) of Ligands		
	Ribavirin	Remdesivir	Velpatasvir
MMGBSA dG Bind (Coulomb)	-40.94	-64.71	-74.64
Complex Energy	-36497.93	-36633.27	-36625.57
Complex Hbond	-458.95	-459.58	-458.31
Complex Solv GB	-7456.90	-7425.34	-7425.64

### 3.6. FDA-approved antivirals ribavirin, velpatasvir, and remdesivir are potential repurposable drugs for clinical trials to treat MPV via inhibition of MP-DNAP:

All findings from the current study indicate great potential of ribavirin, velpatasvir, and remdesivir to inhibit MP-DNAP. Since all three drugs are already FDA-approved, they can be directly tested in the MPV-infected patients thereby accelerating the process of drug discovery. Known human doses and pharmacology for either of these drugs as explained by Nyström et al., 2019 (for ribavirin), Borgia et al., 2019 (for velpatasvir), and Jorgensen et al., 2020 (for remdesivir) can be useful to take them forward against MPV infection [42-44]. Briefly, ribavirin is known to decrease the synthesis of GTP specifically by limiting access to its endogenous substrate inosine-5-monophosphate required for such synthesis. ultimately leading to the decreased synthesis and lower levels of GTP [45]. Ribavirin works as a mutagen in the target virus to cause an 'error catastrophe' due to increased viral mutations [45]. Velpatasvir works as an antiviral medicine as an inhibitor of the target viral replication complex. Sofosbuvir and velpatasvir work together by preventing the virus that causes hepatitis C from spreading inside the host body. Remdesivir is well known to bind the RdRp protein of SARS-CoV-2 and treat COVID-19.

## 4. Conclusions

Current study could also for the first time could identify the interacting residues for cidofovir and tecovirimat against the experimentally solved structure of MP-DNAP otherwise their mechanism of action was still unknown. dGTP was also found to have the highest affinity for MP-DNAP compared to the three other substrates of this enzyme. Since all the ligands including cidofovir,



tecovirimat, ribavirin, remdesivir, and velpatasvir are binding in the active site and just near the  $Mg^{2+}$ , it can be postulated that use of a metal chelator (like EDTA or its analogues etc.) or reducing the amount of magnesium can block the MPV infection via inhibition of its DNAP activity. Nevertheless, all these outcomes need to be experimentally validated using proper *ex vivo*, or *in vivo* assays which is beyond the scope of current study. Analogues of the three lead drugs can also be evaluated. Till there is any specific vaccine available/discovered against MPV, all these drugs/lead molecules can save several thousands of human lives across the world from this viral infection.

**Author Contributions:** Conceptualization, Shahjahan, J.K.D., and S.K.D.; methodology, Shahjahan and S.K.D.; software, Shahjahan and S.K.D.; validation, Shahjahan and S.K.D.; formal analysis, Shahjahan and S.K.D.; investigation, Shahjahan and S.K.D.; resources, S.K.D.; data curation, Shahjahan and S.K.D.; writing—original draft preparation, Shahjahan and S.K.D.; writing—review and editing, Shahjahan and S.K.D.; visualization, Shahjahan and S.K.D.; supervision, S.K.D.; project administration, S.K.D.; funding acquisition, S.K.D. All authors have read and agreed to the published version of the manuscript.

**Funding:** This research received no external funding.

**Institutional Review Board Statement:** Not applicable.

**Informed Consent Statement:** Not applicable.

**Supplementary Data:** Supplementary Tables 1 and 2; Supplementary Figures 1, 2 and 3.

**Data Availability Statement:** All data included in the manuscript.

**Acknowledgments:** Shahjahan and SKD are thankful to the Schrodinger Inc. for providing us one month's free trial of their virtual screening module using which we could conduct experiments and analyses for the current study. Authors are also thankful to their families. Authors are also grateful to Profs. Suman Kundu, and Prof. BK Thelma from the Department of Genetics of the University of Delhi South Campus, India and Dr. Joy Kumar Dey, CCRH, Ministry of AYUSH, GoI, for their continuous support and scientific discussions to improve the current manuscript. SKD acknowledges financial and infrastructural supports from the University of Delhi (R&D and seed grants), and Dr. B. R. Ambedkar Center for Biomedical Research [ACBR] (start-up and research grants). SKD also acknowledges the Institution of Eminence grant (grant ID: IoE/2021/12/FRP) from the University of Delhi, India for providing financial support. Graphical abstract was made using BioRender (<https://biorender.com>). Shahjahan and SKD are also thankful to Smaranjot Kaur and Iram, ACBR for their continuous encouragement for the current work.

**Conflicts of Interest:** The authors declare no conflict of interest.

## REFERENCES:

- [1] P. Magnus, "VON, ANDEBSON, EK, PETEBSON, KB & ANDEBSON, AB (1959). A pox-like disease in cynomolgus monkeys," *Acta Pathologica et Microbiologica Scandinavica*, vol. 46, pp. 156-76, 1959.
- [2] A. Gessain, E. Nakoune, and Y. Yazdanpanah, "Monkeypox," *New England Journal of Medicine*, vol. 387, no. 19, pp. 1783-1793, 2022.
- [3] A. M. McCollum and I. K. Damon, "Human monkeypox," *Clinical infectious diseases*, vol. 58, no. 2, pp. 260-267, 2014.
- [4] G. Pauli *et al.*, "Orthopox viruses: infections in humans," *Transfusion Medicine and Hemotherapy*, vol. 37, no. 6, p. 351, 2010.
- [5] A. MacNeil *et al.*, "Transmission of atypical varicella-zoster virus infections involving palm and sole manifestations in an area with monkeypox endemicity," *Clinical Infectious Diseases*, vol. 48, no. 1, pp. e6-e8, 2009.
- [6] Z. Ozkurt and E. Ç. Tanrıverdi, "COVID-19: Gastrointestinal manifestations, liver injury and recommendations," *World Journal of Clinical Cases*, vol. 10, no. 4, p. 1140, 2022.
- [7] S. E. F. Yong *et al.*, "Imported Monkeypox, Singapore," *Emerging infectious diseases*, vol. 26, no. 8, p. 1826, 2020.
- [8] A. Vaughan *et al.*, "Two cases of monkeypox imported to the United Kingdom, September 2018," *Eurosurveillance*, vol. 23, no. 38, p. 1800509, 2018.
- [9] F. Anwar *et al.*, "Clinical Manifestation, Transmission, Pathogenesis, and Diagnosis of Monkeypox Virus: A Comprehensive Review," *Life*, vol. 13, no. 2, p. 522, 2023.
- [10] E. De Clercq, "Acyclic nucleoside phosphonates: past, present and future: bridging chemistry to HIV, HBV, HCV, HPV, adeno-, herpes-, and poxvirus infections: the phosphonate bridge," *Biochemical pharmacology*, vol. 73, no. 7, pp. 911-922, 2007.
- [11] J. G. Rizk, G. Lippi, B. M. Henry, D. N. Forthal, and Y. Rizk, "Prevention and treatment of monkeypox," *Drugs*, pp. 1-7, 2022.
- [12] N. Erez *et al.*, "Diagnosis of imported monkeypox, Israel, 2018," *Emerging infectious diseases*, vol. 25, no. 5, p. 980, 2019.
- [13] B. Moss, "Poxvirus DNA replication. Cold Spring Harb Perspect Biol 5: a010199," ed, 2013.

- [14] J. R. Kugelman *et al.*, "Genomic variability of monkeypox virus among humans, Democratic Republic of the Congo," *Emerging infectious diseases*, vol. 20, no. 2, p. 232, 2014.
- [15] P. L. Earl, E. V. Jones, and B. Moss, "Homology between DNA polymerases of poxviruses, herpesviruses, and adenoviruses: nucleotide sequence of the vaccinia virus DNA polymerase gene," *Proceedings of the National Academy of Sciences*, vol. 83, no. 11, pp. 3659-3663, 1986.
- [16] E. V. Jones and B. Moss, "Mapping of the vaccinia virus DNA polymerase gene by marker rescue and cell-free translation of selected RNA," *Journal of virology*, vol. 49, no. 1, pp. 72-77, 1984.
- [17] P. Traktman, P. Sridhar, R. C. Condit, and B. E. Roberts, "Transcriptional mapping of the DNA polymerase gene of vaccinia virus," *Journal of virology*, vol. 49, no. 1, pp. 125-131, 1984.
- [18] J. Luczkowiak, M. Álvarez, A. Sebastián-Martín, and L. Menéndez-Arias, "DNA-dependent DNA polymerases as drug targets in herpesviruses and poxviruses," *Viral Polymerases*, pp. 95-134, 2019.
- [19] M. Ahmad *et al.*, "Prediction of small molecule inhibitors targeting the severe acute respiratory syndrome coronavirus-2 RNA-dependent RNA polymerase," *ACS omega*, vol. 5, no. 29, pp. 18356-18366, 2020.
- [20] B. K. Biswal *et al.*, "Non-nucleoside inhibitors binding to hepatitis C virus NS5B polymerase reveal a novel mechanism of inhibition," *Journal of molecular biology*, vol. 361, no. 1, pp. 33-45, 2006.
- [21] B. K. Biswal *et al.*, "Crystal structures of the RNA-dependent RNA polymerase genotype 2a of hepatitis C virus reveal two conformations and suggest mechanisms of inhibition by non-nucleoside inhibitors," *Journal of Biological Chemistry*, vol. 280, no. 18, pp. 18202-18210, 2005.
- [22] S. K. Dey *et al.*, "Suramin, penciclovir, and anidulafungin exhibit potential in the treatment of COVID-19 via binding to nsp12 of SARS-CoV-2," *Journal of Biomolecular Structure and Dynamics*, pp. 1-17, 2021.
- [23] R. Sah *et al.*, "Public health emergency of international concern declared by the world health organization for monkeypox," *Global Security: Health, Science and Policy*, vol. 7, no. 1, pp. 51-56, 2022.
- [24] S. Kumari, S. Chakraborty, M. Ahmad, V. Kumar, P. B. Tailor, and B. K. Biswal, "Identification of probable inhibitors for the DNA polymerase of Monkeypox virus through the virtual screening approach," *International Journal of Biological Macromolecules*, 2022.
- [25] Q. Peng *et al.*, "Structure of monkeypox virus DNA polymerase holoenzyme," *Science*, vol. 379, no. 6627, pp. 100-105, 2023.
- [26] N. Rahman, Z. Basharat, M. Yousuf, G. Castaldo, L. Rastrelli, and H. Khan, "Virtual screening of natural products against type II transmembrane serine protease (TMPRSS2), the priming agent of coronavirus 2 (SARS-CoV-2)," *Molecules*, vol. 25, no. 10, p. 2271, 2020.
- [27] K. H. Chowdhury *et al.*, "Drug repurposing approach against novel coronavirus disease (COVID-19) through virtual screening targeting SARS-CoV-2 main protease," *Biology*, vol. 10, no. 1, p. 2, 2020.
- [28] R. Roy, M. F. Sk, N. A. Jonniya, S. Poddar, and P. Kar, "Finding potent inhibitors against SARS-CoV-2 main protease through virtual screening, ADMET, and molecular dynamics simulation studies," *Journal of Biomolecular Structure and Dynamics*, pp. 1-13, 2021.
- [29] S. K. Dey *et al.*, "Suramin, Penciclovir and Anidulafungin bind nsp12, which governs the RNA-dependent-RNA polymerase activity of SARS-CoV-2, with higher interaction energy than Remdesivir, indicating potential in the treatment of Covid-19 infection," *OSF Preprints. doi*, vol. 10, 2020.
- [30] B. Farasati Far *et al.*, "Metronidazole, acyclovir and tetrahydrobiopterin may be promising to treat COVID-19 patients, through interaction with interleukin-12," *Journal of Biomolecular Structure and Dynamics*, pp. 1-19, 2022.
- [31] S. K. Saxena, *Coronavirus disease 2019 (COVID-19): epidemiology, pathogenesis, diagnosis, and therapeutics*. Springer nature, 2020.
- [32] M. E. Mahfouz *et al.*, "Comparison of Different Antiviral Regimens in the Treatment of Patients with Severe COVID-19: A Retrospective Cohort," *Medicina*, vol. 59, no. 2, p. 260, 2023.

- [33] T. Ertan-Bolelli, K. Bolelli, S. D. Elçi, and F. B. Belen-Apak, "Promising drug Fondaparinux for the treatment of Covid-19: An in silico analysis of low molecular weight heparin, direct oral anticoagulant, and antiplatelet drug interactions with host protease furin," *Cardiovascular Drugs and Therapy*, pp. 1-8, 2022.
- [34] E. F. Pettersen, T. D. Goddard, C. C. Huang, G. S. Couch, D. M. Greenblatt, and E. C. Meng, "UCSF Chimera—a visualization system for exploratory research and analysis.," *Journal of Computational Chemistry*, vol. 25, no. 13, pp. 1605-12, 2004.
- [35] L. Schrodinger, "Schrodinger software suite. New York: Schrödinger, LLC," vol. 670, 2011.
- [36] A. Grosdidier, V. Zoete, and O. Michielin, " SwissDock, a protein-small molecule docking web service based on EADock DSS.," *Nucleic Acids Research*, vol. 39, no. Web Server issue, pp. W270–W277, 2011.
- [37] A. Waterhouse *et al.*, "SWISS-MODEL: homology modelling of protein structures and complexes," *Nucleic Acids Research*, vol. 46, no. W1, pp. W296-W303, 2018.
- [38] S. Rosignoli and A. Paiardini, "Boosting the full potential of PyMOL with structural biology plugins," *Biomolecules*, vol. 12, no. 12, p. 1764, 2022.
- [39] J. Li, R. Abel, K. Zhu, Y. Cao, S. Zhao, and R. A. Friesner, "The VSGB 2.0 model: a next generation energy model for high resolution protein structure modeling," *Proteins: Structure, Function, and Bioinformatics*, vol. 79, no. 10, pp. 2794-2812, 2011.
- [40] E. Wang *et al.*, "VAD-MM/GBSA: A Variable Atomic Dielectric MM/GBSA Model for Improved Accuracy in Protein–Ligand Binding Free Energy Calculations," *Journal of Chemical Information and Modeling*, vol. 61, no. 6, pp. 2844-2856, 2021.
- [41] S. Chakraborty *et al.*, "Clinical management, antiviral drugs and immunotherapeutics for treating monkeypox. An update on current knowledge and futuristic prospects," *International Journal of Surgery (London, England)*, vol. 105, p. 106847, 2022.
- [42] K. Nyström, J. Waldenström, K.-W. Tang, and M. Lagging, "Ribavirin: pharmacology, multiple modes of action and possible future perspectives," *Future Virology*, vol. 14, no. 3, pp. 153-160, 2019.
- [43] S. M. Borgia *et al.*, "Sofosbuvir/velpatasvir for 12 weeks in hepatitis C virus-infected patients with end-stage renal disease undergoing dialysis," *Journal of hepatology*, vol. 71, no. 4, pp. 660-665, 2019.
- [44] S. C. Jorgensen, R. Kebriaei, and L. D. Dresser, "Remdesivir: review of pharmacology, pre-clinical data, and emerging clinical experience for COVID-19," *Pharmacotherapy: The Journal of Human Pharmacology and Drug Therapy*, vol. 40, no. 7, pp. 659-671, 2020.
- [45] E. Thomas, M. G. Ghany, and T. J. Liang, "The application and mechanism of action of ribavirin in therapy of hepatitis C," *Antiviral Chemistry and Chemotherapy*, vol. 23, no. 1, pp. 1-12, 2012.